Radiology

ORIGINAL RESEARCH ■ PEDIATRIC IMAGING

Radiation Dose Reduction with Hybrid Iterative Reconstruction for Pediatric CT[1]

Sarabjeet Singh, MD
Mannudeep K. Kalra, MD
Anuradha S. Shenoy-Bhangle, MD
Aashna Saini
Debra A. Gervais, MD
Sjirk J. Westra, MD
James H. Thrall, MD

Purpose: To assess image quality and radiation dose reduction with hybrid iterative reconstruction of pediatric chest and abdominal computed tomographic (CT) data compared with conventional filtered back projection (FBP).

Materials and Methods: A total of 234 patients (median age, 12 years; age range, 6 weeks to 18 years) underwent chest and abdominal CT in this institutional review board–approved HIPAA-compliant retrospective study. CT was performed with a hybrid adaptive statistical iterative reconstruction (ASIR)-enabled 64–detector row CT scanner. Scanning protocols were adjusted for clinical indication and patient weight to enable acquisition of reduced-dose CT images in all patients, and tube current was further lowered for ASIR protocols. Weight, age, and sex were recorded, and objective noise was measured in the descending thoracic aorta for chest CT and in the liver for abdominal CT. Of the 234 consecutive patients who underwent ASIR-enabled CT (115 chest and 119 abdominal examinations), 70 patients had undergone prior FBP CT. ASIR and FBP CT studies (29 chest and 41 abdominal studies) in these 70 patients were reviewed for image quality, artifacts, and diagnostic confidence by two pediatric radiologists working independently. Data were analyzed with multiple paired *t* tests.

Results: Compared with FBP, ASIR enabled dose reduction of 46.4% (3.7 vs 6.9 mGy) for chest CT and 38.2% (5.0 vs 8.1 mGy) for abdominal CT ($P < .0001$). Both radiologists deemed image quality of and diagnostic confidence with ASIR and FBP CT images as acceptable, without any artifacts. Despite the lower radiation dose used, ASIR images (chest, 10.7 ± 2.5 [mean ± standard deviation]; abdomen, 11.8 ± 3.4) had substantially less objective noise than did FBP images (chest, 13.3 ± 3.8; abdomen, 13.8 ± 5.2) ($P = .001$, $P = .006$, respectively).

Conclusion: Use of a hybrid iterative reconstruction technique, such as ASIR, enables substantial radiation dose reduction for pediatric CT when compared with FBP and maintains image quality and diagnostic confidence.

Supplemental material: *http://radiology.rsna.org/lookup/suppl/doi:10.1148/radiol.12110268/-/DC1*

[1] From the Department of Radiology, Massachusetts General Hospital, 25 New Chardon St, 4th Floor, Boston MA 02114. Received February 6, 2011; revision requested March 28; revision received July 28; accepted September 16; final version accepted December 29. **Address correspondence to** S.S. (e-mail: *ssingh@partners.org*).

Over the past decade, concerns about radiation dose associated with computed tomography (CT), especially in children, have been highlighted (1–3). Many of the concerns stem from the rapid increase in the number of CT scans performed worldwide and the corresponding increase in radiation exposure to the population (4). While contemporary multidetector row CT offers a noninvasive and convenient way of obtaining information that can benefit patient care and outcome, frequent scanning leads to increased risk of radiation-induced carcinogenesis (5).

In response to these concerns and calls for dose reduction, CT vendors have developed several techniques to help maintain diagnostic image quality of studies acquired at a lower radiation dose (6). Automatic exposure control (7–10) and hybrid iterative reconstruction, such as adaptive statistical iterative reconstruction (ASIR) and iterative reconstruction in image space, are two of the techniques aimed at reducing image noise. While the use of various automatic exposure control techniques in both adults and children has been reported (7–10), the utility of hybrid iterative reconstruction techniques in radiation dose reduction strategies—primarily for chest and abdominal CT—has been documented in only adult patients (11–17).

The purpose of our study was to assess image quality and radiation dose reduction with hybrid iterative reconstruction of pediatric chest and abdominal CT data compared with conventional filtered back projection (FBP).

Advances in Knowledge

- Adaptive statistical iterative reconstruction (ASIR) enables 46.4% (3.7 vs 6.9 mGy) and 38.2% (5.0 vs 8.1 mGy) radiation dose reduction for pediatric chest and abdomen CT, respectively, when compared with filtered back projection (FBP).
- Radiation dose used with ASIR was lower than that used with FBP; however, subjective image quality with ASIR was equal to or better than that with FBP.
- Despite substantial dose reduction, ASIR-enabled CT had 14.5% (11.8 vs 13.8) lower objective noise for abdominal CT and 19.5% (10.7 vs 13.3) lower noise for chest CT than did corresponding FBP-enabled CT.

Materials and Methods

Patients

This retrospective observational study was approved by the institutional review board of our human research committee and was compliant with the Human Insurance Portability and Accountability Act. The institutional review board waived the need to obtain informed consent for this retrospective analysis of data.

All consecutive pediatric patients who underwent routine chest and abdominal CT with ASIR-based protocols and a 64–detector row CT scanner (GE Discovery CT 750 HD; GE Healthcare, Waukesha, Wis) capable of ASIR reconstruction from January 1, 2009, to July 31, 2010, were included in this study. Patients examined with protocols that were noncompliant with ASIR-based CT protocols were excluded. This study comprised 115 chest and 119 abdominal ASIR-enabled CT examinations performed in 234 patients 18 years old or younger with routine or emergent clinical indications. Of these 234 patients, 70 had undergone prior CT with FBP reconstruction (chest CT, n = 29; abdominal CT, n = 41) (Fig 1) performed less than 1 year prior to CT with ASIR reconstruction. Two pediatric patients who underwent chest CT during this interval were excluded because of noncompliance with the ASIR-based CT protocols.

Implication for Patient Care

- The use of ASIR-enabled and indication-based protocols yields reduced image noise in lower-radiation-dose pediatric chest and abdominal CT examinations.

Weight was recorded on the CT user interface for all patients just prior to scanning and was archived in the picture archiving and communication system (Impax ES; AGFA Technical Imaging Systems, Ridgefield Park, NJ). Patients were weighed on a digital scale in the CT suite, or parents were asked about their child's weight just prior to CT scanning.

The most common indications for chest CT were nonresolving or complicated pneumonia (58 of 115 patients), staging or restaging of known cancer (25 of 115 patients), nonresolving or loculated pleural effusions (eight of 115 patients), and cystic fibrosis (three of 115 patients). The most common indications for abdominal CT were abdominal pain (76 of 119 patients), staging or restaging of known cancer (22 of 119 patients), appendicitis (11 of 119 patients), and inflammatory bowel disease (seven of 119 patients).

CT Equipment and Scanning Protocols

All CT reconstructions with ASIR were performed with the aforementioned 64-detector row CT scanner.

The pediatric scanning protocols used in our study with FBP-based CT reconstruction have been reported in

Published online before print
10.1148/radiol.12110268 **Content codes:** PD CT

Radiology 2012; 263:537–546

Abbreviations:
ASIR = adaptive statistical iterative reconstruction
$CTDI_{vol}$ = volume CT dose index
DLP = dose-length product
FBP = filtered back projection

Author contributions:
Guarantor of integrity of entire study, M.K.K.; study concepts/study design or data acquisition or data analysis/interpretation, all authors; manuscript drafting or manuscript revision for important intellectual content, all authors; approval of final version of submitted manuscript, all authors; literature research, S.S., M.K.K.; clinical studies, S.S., M.K.K., A.S., S.W.; experimental studies, S.S., A.S.; statistical analysis, S.S., M.K.K., A.S.S.; and manuscript editing, S.S., M.K.K., S.J.W., J.H.T.

Potential conflicts of interest are listed at the end of this article.

a prior publication (19). Scanning parameters for each indication zone and weight subgroup for CT data reconstructed with FBP and ASIR are summarized in Table E1 (online). Instead of six indication categories reported in our prior study, our simplified pediatric protocols had only four indication categories, or zones, for both ASIR- and FBP-enabled CT at the time of this study. We excluded the indication category for CT angiography, as only one child in this category underwent CT. Also, our protocols did not have a separate higher-radiation-dose indication category or a specific kidney stone category. Instead, patients suspected of having kidney stones were examined with the green zone protocol, which was also used for index chest CT (without concomitant abdominal CT) and the first follow-up abdominal CT examination. Subjects who were undergoing index abdominal CT or combined chest and abdominal CT were examined with pink zone protocols. Subjects who had undergone one prior chest CT examination or more than one prior abdominal CT examination were scanned with the red zone protocol, as were subjects who were being evaluated for musculoskeletal indications, such as spine or chest wall deformities. Within each indication zone, scanning parameters were stratified on the basis of patient weight (0–9 kg, 10–26 kg, 27–45 kg, 46–100 kg, and ≥101 kg).

Fundamentals of FBP- and ASIR-based image reconstruction are summarized in Appendix E1 (online). For further details, readers are encouraged to refer to prior publications on use of ASIR in adult patients (11–17).

Since ASIR is an image reconstruction technique used to lower image noise, we reduced radiation dose a priori with adjustment in automatic exposure control technique to obtain lower-radiation-dose data, which were then reconstructed with ASIR. To enable an approximately 30% dose reduction with use of ASIR 30% blending, on the basis of the vendor's suggestion, we increased noise indexes by multiplying them by 1.2 and decreased minimum and maximum tube current by multiplying them by 0.8 and rounding to the nearest multiple of ten. Noise index and minimum and maximum tube current are components of the combined longitudinal and transverse automatic exposure control technique (AutomA 3D; GE Healthcare) used in our study. This technique automatically adjusts tube current on the basis of the patient's region attenuation and thickness in the *x* and *y* axes of tube rotation and along the *z* axis or longitudinal scanning direction. For this tube current modulation to occur, the system requires users to specify a desired image quality or image noise (noise index is a descriptor of this entity) and the range of tube current for modulation. The peak voltage (80–120 kVp) was kept similar for CT images reconstructed with FBP and ASIR techniques.

All CT images reconstructed with FBP used a standard soft-tissue reconstruction kernel for the abdomen and a detailed reconstruction kernel for the chest. The same kernel was used for CT images reconstructed with ASIR at 30% ASIR-FBP blending proportion. For both ASIR- and FBP-enabled CT image reconstruction, all other scanning parameters were held constant at 64 × 0.625-mm detector configuration, 40-mm table speed per gantry rotation, 0.5-second gantry rotation time, 0.984:1 beam pitch, 5-mm reconstructed section thickness, and 5-mm intersection interval for abdominal CT and 2.5-mm reconstructed section thickness and 2.5-mm intersection interval for chest CT.

Figure 1

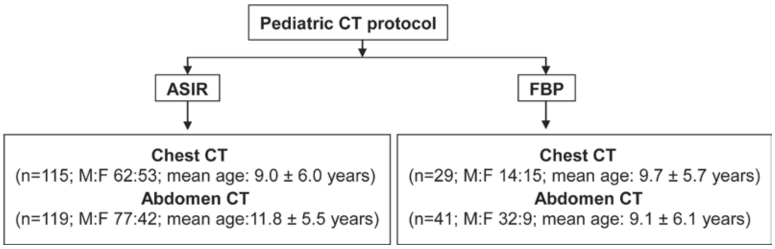

Figure 1: Flowchart summarizes characteristics of pediatric patients who underwent chest or abdominal ASIR- or FBP-enabled CT. *M:F* = male-to-female ratio, *n* = number of CT examinations.

Quantitative Assessment

Maximum transverse diameter was measured for all CT studies from a transverse chest CT image at the level of the tracheal carina and from a transverse abdominal CT image at the level of the upper pole of the right kidney. This measurement was obtained by using electronic calipers available in our PACS user interface.

Circular regions of interest of at least 1 cm^2 were drawn in the descending thoracic aorta, carina, and anterior chest wall muscles at the level of tracheal bifurcation to obtain quantitative image noise, which represents standard deviation of the mean Hounsfield units. Large circular regions of interest that measured at least 3 cm^2 and 1 cm^2 were drawn in homogeneous regions of the right and left hepatic lobes and in the abdominal aorta, respectively, to measure abdominal image noise at the level of the porta hepatis. An author (S.S., 3 years of experience in dose reduction research) placed the regions of interest and did not evaluate qualitative image quality to avoid bias. Mean CT numbers from these regions of interests were also recorded (Fig E2 [online]).

To estimate dose difference between ASIR- and prior FBP-enabled CT examinations, we recorded the volume CT dose index ($CTDI_{vol}$) in milligrays and the dose-length product (DLP) in milligray-centimeters for all CT examinations from the dose information page. Given the wide range of patient sizes in our study and to adjust for phantom size, we recorded phantom size (16- or 32-cm body phantom) used for estimation of $CTDI_{vol}$ and DLP.

Table 1

Measurements on Pediatric Chest and Abdominal CT Images Reconstructed with ASIR and Further Stratified by Colored Zones and Weight

Examination Group, Zone, and Weight	No. of Patients	Age (y)	Weight (kg)	Maximum Transverse Diameter (cm)	$CTDI_{vol}$ (mGy)*†	DLP (mGy·cm)*
Chest CT						
Overall	115	9 (12)	24.5 (41.3)	24.7 (11.7)	3.7 ± 1.4	153.2 ± 103.4
Zone						
Pink	35	10 (11.3)	27 (48.1)	26.8 (14.8)	5.5 ± 1.4	222.6 ± 125.5
Green	64	7 (12)	22 (40)	23.7 (10.9)	4.2 ± 1.4	133.8 ± 78.9
Red	16	10.5 (6)	29 (26)	27.5 (8)	2.4 ± 0.6	78.9 ± 25.2
Weight						
0–9 kg	17	0.9 (1.7)	8 (3)	16.4 (3.1)	2.5 ± 0.4	55.5 ± 41.7
10–26 kg	49	4 (4)	18 (8)	21.7 (3.6)	4.5 ± 1.1	129.0 ± 64.6
27–45 kg	12	10.5 (4.2)	40 (6)	28.5 (2.8)	3.3 ± 1.6	156.5 ± 115.3
46–100 kg	36	16 (3)	62.5 (20.3)	34.8 (5.8)	5.1 ± 1.5	227.5 ± 110.7
>101 kg	1	16.0 (NA)	138.0 (NA)	45.5 (NA)	9.8	279.9
Abdominal CT						
Overall	119	13 (11)	41 (40)	25 (9.4)	5.7 ± 1.8	258.2 ± 116.7
Zone						
Pink	84	15 (7)	48.5 (42.2)	26.4 (9.9)	6.1 ± 1.7	283.6 ± 117.0
Green	30	7 (13)	23 (35.5)	22.2 (7.4)	4.8 ± 1.0	214.6 ± 88.7
Red	5	8 (6)	28 (21)	20.7 (1.5)	2.5 ± 0.6	99.2 ± 28.5
Weight						
0–9 kg	0	...	...	...	....	...
10–26 kg	42	5 (3.2)	18 (5)	19.8 (1.5)	5.2 ± 1.2	189.5 ± 50.3
27–45 kg	20	12 (4)	40 (7)	23.8 (4.6)	4.8 ± 1.5	222.4 ± 85.4
46–100 kg	50	17 (3)	59 (15.5)	29.2 (4.4)	5.8 ± 1.1	297.2 ± 94.7
>101 kg	7	18 (1)	95.5 (20.2)	93.5 (45.1)	10.5 ± 3.0	545.8 ± 147.5

Note.—Unless otherwise indicated, data are median number of patients, and data in parentheses are the interquartile range.

* Data are mean ± standard deviation.

† Phantom size of 16 cm was used to estimate $CTDI_{vol}$ for chest and abdominal CT in children who weighed less than 26 kg.

In addition, we recorded the average tube current used in each CT examination included in our study. All images of each CT study were reviewed for presence (tube current modulation with automatic exposure control) or absence (no tube current modulation with automatic exposure control) of fluctuation in tube current. We recorded the highest and lowest tube current, as well as the tube current values in between, to determine average tube current. We classified CT examinations in both ASIR and FBP groups on the basis of presence or absence of change in tube current with use of tube current modulation. Absence of tube current modulation was defined as scanning of the entire region at either minimum (when tube current modulation is limited at the minimum current) or at maximum (when tube current modulation saturates at maximum current) tube current.

Qualitative Assessment

Qualitative assessment of image quality was performed in 70 patients who had both ASIR CT images and prior CT images obtained in the same region with FBP-enabled CT image reconstruction (chest CT, n = 29; abdominal CT, n = 41). These transverse CT images were reviewed independently for image quality and lesion assessment on two calibrated monitors at the picture archiving and communication system workstation by two pediatric radiologists (S.J.W., A.S.S.; 23 and 3 years of experience, respectively). At the time of image quality assessment, all scanning and reconstruction settings were removed from the display monitors to facilitate blinded evaluation of image quality, and FBP and ASIR images were reviewed side by side. Abdominal CT images were displayed with standard soft-tissue window settings (window width, 400 HU; window length, 40 HU); however, for chest CT images, lesion detection and visibility of small structures was evaluated with lung (window width, 1500 HU; window length, −600 HU) and mediastinal soft-tissue (window width, 400 HU; window length, 40 HU) window settings. Radiologists were allowed to change the window settings to suit their individual preferences, and standard picture archiving and communication system tools (image magnification and panning) were

Table 2

Measurements on Pediatric Chest and Abdominal CT Images Reconstructed with ASIR amd FBP

Parameter	ASIR with Prior FBP	FBP	*P* Value
Chest CT			
No. of cases	29	29	
Age (y)	10 (10)*	9 (12)	.47
Weight (kg)	29 (43)*	30 (39.5)	.20
Maximum transverse diameter (cm)	28 (9.7)*	23.5 (13.1)	.38
$CTDI_{vol}$ (mGy)	3.7 ± 1.4*†	6.9 ± 2.0†	<.0001
DLP (mGy·cm)	121.2 ± 73.0*†	204.0 ± 118.2†	<.0001
Abdominal CT			
No. of cases	41	41	
Age (y)	7 (11)*	5 (9.7)	.72
Weight (kg)	22 (31.8)*	20 (32.8)	.2
Maximum transverse diameter (cm)	20.4 (7.2)*	20.9 (9.2)	.75
CTDIvol (mGy)	5.0 ± 1.2*†	8.1 ± 2.2†	<.0001
DLP (mGy·cm)	216.8 ± 94.4*†	327.9 ± 128.0†	<.0001

Note.—Unless otherwise indicated, data are the median, and data in parentheses are the interquartile range.

* Quantitative variables, multiple paired *t* test.

† Data are mean ± standard deviation.

made available to them for detailed evaluation of chest and abdominal CT studies. Each radiologist independently graded ASIR and FBP CT images for *(a)* subjective noise on a five-point scale (1, very little noise, minimal noise, or no noise; 2, noise present but less than average; 3, average noise; 4, greater-than-average noise; 5, unacceptably high noise); *(b)* visibility of small structures on a five-point scale (1, excellent visibility of small and subtle structures of chest or abdomen; 5, unacceptable poor visibility of small or subtle thoracic or abdominal structures); *(c)* diagnostic confidence on a four-point scale (1, completely confident; 2, probably confident; 3, confidence only in limited condition; 4, unacceptably low confidence); *(d)* lesion detection, including number of lesions and their size and conspicuity, on a five-point scale (1, well-seen lesion with well-defined margins; 5, definite artifact mimicking a lesion); and *(e)* image artifacts on a two-point scale (1, no artifacts; 2, artifacts present). Artifacts—including beam hardening, blotchy or pixilated appearance, and different texture of images—were assessed. Image artifacts from motion, metallic implants, or placement of arms by the side of imaged body portions were excluded from evaluation. The higher-radiation-dose CT images reconstructed with the FBP technique were considered the reference standard in lesion evaluation.

Statistical Analysis

Data were analyzed by using statistical software (SPSS, version 13.0; SPSS, Chicago, Ill). Average and standard deviations of $CTDI_{vol}$, DLP, mean tube current–time products, weight, transverse diameter, and objective image noise were calculated for CT images reconstructed with ASIR and FBP separately for each indication category and weight subgroup. These quantitative variables were also compared by using multiple paired *t* tests to determine statistical differences between ASIR and FBP-enabled CT image reconstruction in different indication and weight groups. To account for multiple repeated testing in the same patient groups, we used Bonferroni adjustment to define a *P* value of less than .007 *(www.quantitativeskills.com/sisa/calculation/Bonfer.php)*. In addition, we compared patient weights, $CTDI_{vol}$, and DLP and presence and absence of tube current modulation for both techniques. Median image quality and lesion assessment scores were estimated for each technique. We did not perform pre or post hoc power analysis, which may have limited the power of our study. Interobserver agreement was determined by using the κ test, and confidence interval of interobserver agreement was selected as 95%.

Results

Patient Distribution

Distribution of patients in different indication categories and weight groups for chest and abdominal CT images reconstructed with the ASIR technique is summarized in Tables 1 and 2.

Image Quality

Details of lesion detection and image noise are summarized in Tables 3 and 4. There was no significant difference in overall Hounsfield units between FBP and ASIR chest and abdominal CT images. Despite significantly lower radiation dose associated with CT images reconstructed with the ASIR technique as compared with those reconstructed with the FBP technique, both radiologists found there were no substantial differences in subjective image quality metrics, including lesion conspicuity, diagnostic confidence, and conspicuity of small structures in abdominal and thoracic CT images (statistical comparison not reported) (κ = 1) (Figs 2, 3, E2, E3 [online]). No image artifacts were found on ASIR or FBP CT images. In most patients, ASIR images had equal or slightly lower image noise than did FBP images.

Radiation Dose

Incidentally, abdominal CT images reconstructed with ASIR were obtained in heavier patients when compared with chest CT images reconstructed with ASIR (mean weight, 43.4 kg ± 24.7 vs 34.6 kg ± 26.4) (*P* = .01), whereas there was no difference in the mean weight of patients who underwent FBP-based chest and abdominal CT (*P* = .2). However, radiation doses with FBP and ASIR chest CT were substantially lower than corresponding radiation doses with abdominal CT (*P* < .0001).

There was a significant difference between $CTDI_{vol}$ and DLP associated with overall ASIR and FBP image reconstruction of chest ($P < .0001$) and abdominal ($P < .0001$) CT images in all indication categories and weight groups. The highest dose reduction with ASIR chest CT compared with that with FBP chest CT was noted in the green (39.1%, 4.2 vs 6.9 mGy) and pink (31.4%, 6.1 vs 8.9 mGy) zone indication categories for abdominal CT ($P < .0001$). Likewise, subjects who weighed 27–45 kg had greater radiation dose reduction (63.7%, 3.3 vs 9.1 mGy) with ASIR chest CT than with FBP chest CT ($P < .0001$). For abdominal CT, the lowest radiation dose (28.3%, 5.8 vs 8.1 mGy) was noted in subjects who weighed 46–100 kg for whom ASIR-assisted CT image reconstruction was performed.

Dose Modulation

Change or fluctuation in tube current was noted in more than half (n = 66, 57.4%) of the 115 patients who underwent ASIR chest CT as compared with slightly less than half (n = 14, 48.2%) of the 29 patients who underwent FBP chest CT (Table E2). There was no change in tube current in most small (0–9-kg) and large (>100-kg) patients who underwent ASIR or FBP chest CT (18 of 19 subjects). Conversely, most patients (70 of 97 patients, 72.2%) in the 10–100-kg group had substantial tube current modulation (12.3–41.8 mAs). Most subjects examined with fluctuating or modulating tube current received a lower radiation dose in the ASIR group ($P < .01$).

For abdominal CT, both FBP and ASIR image reconstruction were associated with a lower radiation dose in all indication categories in the presence of tube current fluctuation ($P < .0001$). Tube current modulation was used in three of the seven patients (weight >101 kg) in whom ASIR-based CT image reconstruction was performed; these three patients received a substantially lower radiation dose than did the four patients examined without tube current adjustment ($P < .0001$) (Table E2). On the other hand, nonmodulated ASIR abdominal CT had lower radiation dose than did tube current–modulated ASIR CT in subjects who weighed

Table 3

Detailed Subjective Image Quality Assessment for Chest and Abdominal CT Images Reconstructed with ASIR and FBP

Findings and Score	ASIR	FBP
Chest CT (n = 29)		
Lesion size		
1	25	25
2	1	1
4	1	1
Lesion conspicuity		
1	27	27
Diagnostic confidence		
1	28	26
2	1	2
3	...	1
Visibility of small structures		
1	25	...
2	4	...
3	...	3
4	...	1
Presence of artifacts	7	7
Severity of artifacts		
2	7	7
Image contrast		
1	5	2
2	4	1
3	20	26
Subjective noise		
2	8	1
3	21	28
Objective noise	10.7 ± 2.5 *†	13.3 ± 3.8*
Abdominal CT (n = 41)		
Lesion size		
1	31	19
2	2	2
4	4	4
Lesion conspicuity		
1	35	35
2	2	2
Diagnostic confidence		
1	40	39
2	1	2
Visibility of small structures		
1	38	38
2	1	1
3	2	2
Presence of artifacts		
2	41	...
4	...	4
Severity of artifacts		
2	2	3
3	...	1
Image contrast		
1	36	36
2	2	2

Table 3 (continues)

Table 3 (continued)

Detailed Subjective Image Quality Assessment for Chest and Abdominal CT Images Reconstructed with ASIR and FBP

Findings and Score	ASIR	FBP
3	3	3
Subjective noise		
2	19	3
3	20	33
4	2	5
Objective noise	11.8 ± 3.4 *†	13.8 ± 5.2*

Note.—Unless otherwise indicated, data are numbers of findings. ASIR technique showed lower subjective and objective image noise for chest and abdominal CT images.

* Data are mean ± standard deviation.

† $P < .05$. Quantitative variables, multiple-paired *t* test with Bonferroni correction.

Table 4

Lesions Detected and CT Findings at Chest and Abdominal CT

Examination and Lesion	No. of Lesions
Chest CT	
Pulmonary nodule	53
Ground-glass opacity	23
Pleural effusion	8
Pulmonary opacity	7
Postoperative scarring	5
Bronchial wall abnormality	4
Other (mediastinal lymph node, pneumomediastinum)	1
Abdominal CT	
Renal cyst	37
Paraortic, ileal, perirectal, mesenteric, or inguinal lymph node	21
Renal calculi	20
Hydronephrosis	6
Bowel wall thickening	6
Ascites	5
Gallbladder stone	4
Cholecystectomy	2
Bilateral ovarian cyst	3
Ovarian tiny high-attenuation lesions	3
Other (nephromegaly, diffuse liver disease, transverse colon stricture, intusseception, pancreatic pseudocyst)	1

27–45 kg, although the difference was not significant ($P = .08$).

None of the FBP or ASIR abdominal or chest CT images had unacceptable image noise or diagnostic confidence, regardless of the presence or absence of tube current modulation (Table 3).

Discussion

Prior studies with iterative reconstruction techniques in phantoms and adult patients have shown promise for dose reduction while maintaining or even enhancing image quality at lower radiation doses (11–15). Prakash et al (14) reported a 25.1% dose reduction with use of abdominal CT and ASIR reconstruction in adults when compared with FBP-based image reconstruction. Similar dose reduction with ASIR has also been reported for chest CT in adults when compared with the FBP technique (11).

In comparison with these adult CT studies with ASIR, we document similar or higher dose reduction with use of ASIR in children (38.2%–46.4%) (13–16).

Furthermore, we found that in comparison with indication- and weight-stratified pediatric CT protocols with the FBP technique in a prior publication, there was additional radiation dose reduction with application of ASIR to an indication- and weight-based pediatric protocol (19).

Another aspect of dose reduction in our study was the effectiveness of the automatic exposure control technique to perform tube current modulation within the narrower ranges of minimum and maximum tube current limits. With application of higher noise index or specification of higher noise in images, we noted higher degree of fluctuation or modulation of tube current for CT images reconstructed with ASIR as compared with those reconstructed with FBP. This was not true for the smallest subjects included in our study because of relatively lower noise index and lower tube current range. Likewise, for the largest subjects in our study (those who weighed more than 101 kg), there was limited fluctuation in tube current; this was conceivably due to inability of the scanner to reach the specified noise indexes within the confines of the specified tube current range. Despite the lack of fluctuation of tube current in a substantial number of patients included in our study, we recommend use of the automatic exposure control technique, as patients with fluctuation in tube current received a lower radiation dose than did patients who underwent scanning without a change in tube current.

As reported in prior studies in adult patients, we found that objective image noise was lower with ASIR than with FBP reconstruction of pediatric chest and abdominal CT images (11–15). A recent phantom study for noise power spectrum analysis has shown that ASIR is associated with lower image noise than FBP at all spatial frequencies (17). However, neither pediatric radiologist noticed any artifacts or alterations in image appearance in any region, including the bony structures, with use of ASIR in pediatric CT examinations, as has been reported in prior studies (11–15). Prakash et al (14) have reported adult CT images reconstructed with ASIR have a blotchy pixilated appearance. Lack of such findings in our study may be due to the fact that pediatric radiologists may have a higher acceptance of image artifacts or noise as compared with radiologists who read adult CT studies. However, it is unlikely that patient size or reconstructed field of view would have led to this lack of alteration in image appearance, as several patients in our study weighed more than 70 kg but did not have any alterations in image texture reported in prior adult studies (11,14).

From the image quality perspective, radiologists did not find any substantial difference in lower-dose ASIR CT images as compared with FBP images despite substantially lower objective noise with the former technique for both chest and abdominal CT. This may be due to the fact that differences in objective noise between ASIR and FBP images were insufficient for visually perceptible change in lesion conspicuity or subjective image noise. Alternatively, because of greater acceptability of image noise among pediatric radiologists at our institution, FBP image reconstructions were deemed acceptable for image interpretation in spite of their higher objective noise.

The chief implication of our study is that it is feasible to apply a hybrid iterative reconstruction technique in children undergoing low-dose chest and abdominal CT. The hybrid iterative reconstruction enables substantial dose reduction with pediatric body CT while maintaining acceptable image quality compared with the conventional FBP technique.

There were limitations in our study. Our study was performed in a retrospective manner but included all consecutive children examined with the ASIR-enabled CT scanner over the course of the study. There was a significant difference in objective image noise ($P < .05$) and radiation doses ($P < .001$) at FBP- and ASIR-reconstructed CT in all weight groups. While we noted no substantial differences in subjective image quality metrics, including lesion conspicuity, diagnostic confidence, and conspicuity of small structures, we did not report any statistical comparisons because of underpowering associated with the low number of cases and events for these measures. Thus, we cannot exclude the possibility of a meaningful difference for these subjective metrics. We did not define the maximum potential for dose reduction with the ASIR technique compared with the FBP technique in children. Not all children with ASIR-based image reconstruction underwent prior CT performed with conventional FBP. Likewise, there was an insufficient number of CT angiographic studies with ASIR, which may have limited application of our study findings to abdominal and thoracic CT angiography. Another limitation of our study was that we did not assess pediatric CT images reconstructed with ASIR that were not compliant with ASIR-specific indication and weight-based stratification. A major reason why we excluded noncompliant pediatric CT studies was that implication of noncompliance with weight- and indication-based protocols has been documented in prior studies (18,19). Also, at our institution, noncompliance at ASIR-enabled CT represented a relatively small fraction of the pediatric CT examinations. We did not calculate the estimated effective doses in these patients, as $CTDI_{vol}$ and DLP are adequate and acceptable dose descriptors with which

Figure 2

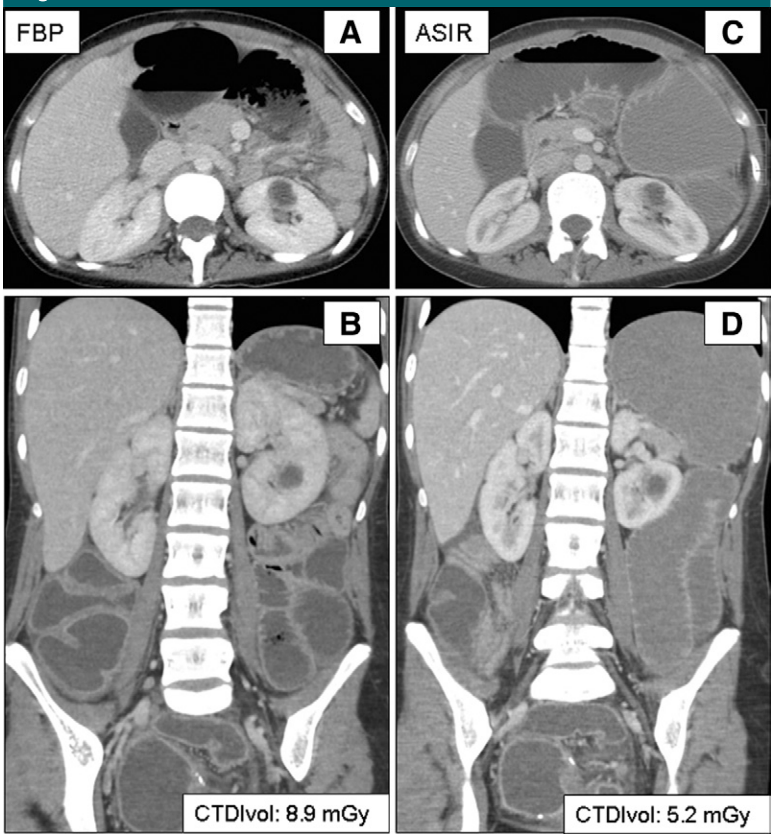

Figure 2: Abdominal CT images in a 17-year-old girl (weight, 39 kg; pink zone) obtained to evaluate possible bowel obstruction after colectomy and J-pouch construction for Crohn disease. *A,* Transverse and, *B,* coronal images reconstructed with FBP (8.9 mGy, 107–189 mA, 120 kVp) show numerous dilated fluid-filled small-bowel loops and 1.6-cm left renal hypodensity. Follow-up, *C,* transverse and, *D,* coronal images reconstructed with ASIR (5.2 mGy, 75–150 mA, 120 kVp) resulted in 41.5% $CTDI_{vol}$ reduction and did not affect lesion detection or image quality.

Figure 3

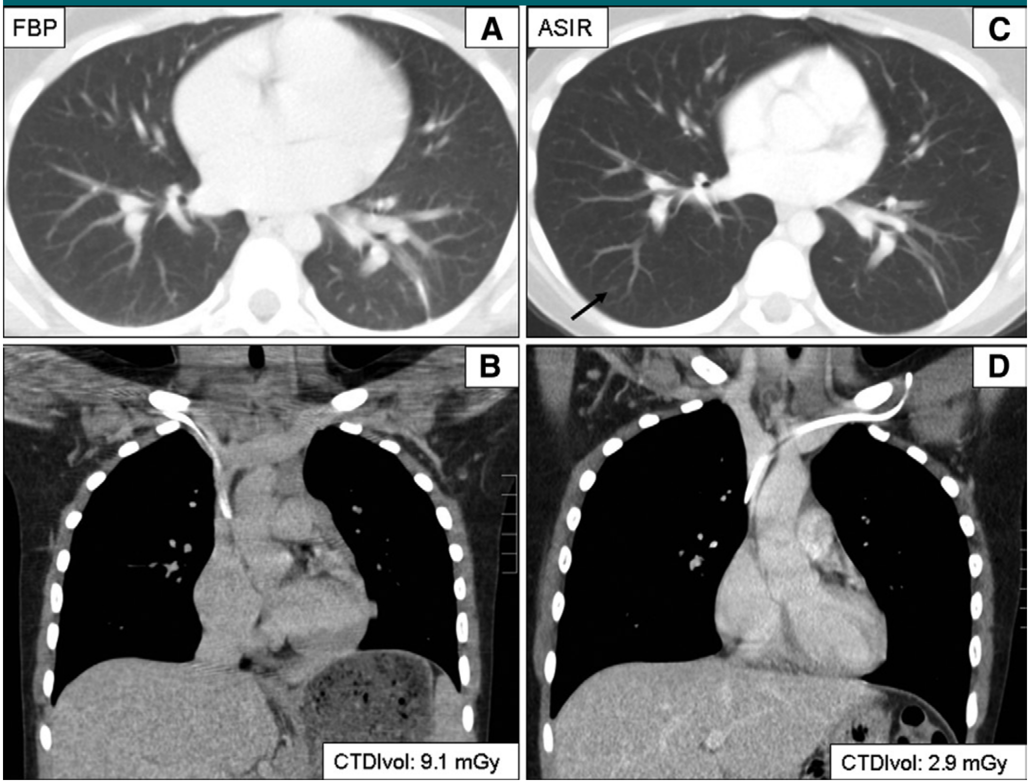

Figure 3: Chest CT images in a 10-year-old girl (weight, 37 kg; green zone) with a known history of rhabdomyodarcoma *A,* Transverse and, *B,* coronal images reconstructed with FBP (9.1 mGy, 88 mA, 120 kVp). Follow-up, *C,* transverse and, *D,* coronal images reconstructed with ASIR (2.9 mGy, 55 mA, 120 kVp) show ill-defined ground-glass opacity (arrow) and resulted in 68% $CTDI_{vol}$ reduction when compared with prior FBP images.

to compare radiation dose between CT examinations. Another limitation of our study was that we did not compare ASIR- and FBP-enabled image reconstructions at the same radiation dose levels or in the same CT examinations. The primary reason for this was that since the examination was performed in a retrospective manner, in most cases either the ASIR or the FBP reconstruction was not available. Thus, we did not evaluate the true diagnostic performance with an independent reference standard.

In conclusion, ASIR-enabled and indication-based protocols reduce image noise in lower-radiation-dose pediatric chest and abdomen CT examinations when compared with FBP.

Disclosures of Potential Conflicts of Interest: **S.S.** No potential conflicts of interest to disclose. **M.K.K.** Financial activities related to the present article: institution received a research grant from GE Healthcare. Financial activities not related to the present article: received an honorarium for continued education talks from GE Healthcare. Other relationships: none to disclose. **A.S.S.** No potential conflicts of interest to disclose. **A.S.** No potential conflicts of interest to disclose. **D.A.G.** No potential conflicts of interest to disclose. **S.J.W.** No potential conflicts of interest to disclose. **J.H.T.** No potential conflicts of interest to disclose.

References

1. Brenner D, Elliston C, Hall E, Berdon W. Estimated risks of radiation-induced fatal cancer from pediatric CT. AJR Am J Roentgenol 2001;176(2):289–296.
2. Huda W, Atherton JV, Ware DE, Cumming WA. An approach for the estimation of effective radiation dose at CT in pediatric patients. Radiology 1997;203(2):417–422.
3. Frush DP, Donnelly LF. Helical CT in children: technical considerations and body applications. Radiology 1998;209(1):37–48.
4. IMV Medical Information Division. 2006 CT market summary report. Des Plaines, Ill: IMV Medical Information Division, 2006.
5. Hollingsworth C, Frush DP, Cross M, Lucaya J. Helical CT of the body: a survey of techniques used for pediatric patients. AJR Am J Roentgenol 2003;180(2):401–406.
6. Kalra MK, Maher MM, Toth TL, et al. Strategies for CT radiation dose optimization. Radiology 2004;230(3):619–628.
7. Kalra MK, Maher MM, Toth TL, Kamath RS, Halpern EF, Saini S. Radiation from "extra" images acquired with abdominal and/or pelvic CT: effect of automatic tube current modulation. Radiology 2004;232(2):409–414.
8. Kalra MK, Maher MM, Toth TL, Kamath RS, Halpern EF, Saini S. Comparison of z-axis automatic tube current modulation technique with fixed tube current CT scanning of abdomen and pelvis. Radiology 2004;232(2):347–353.
9. Kalra MK, Maher MM, Kamath RS, et al. Sixteen-detector row CT of abdomen and

pelvis: study for optimization of z-axis modulation technique performed in 153 patients. Radiology 2004;233(1):241–249.

10. Kalra MK, Maher MM, D'Souza RV, et al. Detection of urinary tract stones at low-radiation-dose CT with z-axis automatic tube current modulation: phantom and clinical studies. Radiology 2005;235(2):523–529.

11. Prakash P, Kalra MK, Ackman JB, et al. Diffuse lung disease: CT of the chest with adaptive statistical iterative reconstruction technique. Radiology 2010;256(1):261–269.

12. Flicek KT, Hara AK, Silva AC, Wu Q, Peter MB, Johnson CD. Reducing the radiation dose for CT colonography using adaptive statistical iterative reconstruction: a pilot study. AJR Am J Roentgenol 2010;195(1):126–131.

13. Hara AK, Paden RG, Silva AC, Kujak JL, Lawder HJ, Pavlicek W. Iterative reconstruction technique for reducing body radiation dose at CT: feasibility study. AJR Am J Roentgenol 2009;193(3):764–771. [Published correction appears in AJR Am J Roentgenol 2009;193(4):1190.]

14. Prakash P, Kalra MK, Kambadakone AK, et al. Reducing abdominal CT radiation dose with adaptive statistical iterative reconstruction technique. Invest Radiol 2010;45(4):202–210.

15. Singh S, Kalra MK, Hsieh J, et al. Abdominal CT: comparison of adaptive statistical iterative and filtered back projection reconstruction techniques. Radiology 2010;257(2):373–383.

16. Heilbron BG, Leipsic J. Submillisievert coronary computed tomography angiography using adaptive statistical iterative reconstruction: a new reality. Can J Cardiol 2010;26(1):35–36.

17. Marin D, Nelson RC, Schindera ST, et al. Low-tube-voltage, high-tube-current multidetector abdominal CT: improved image quality and decreased radiation dose with adaptive statistical iterative reconstruction algorithm—initial clinical experience. Radiology 2010;254(1):145–153.

18. Frush DP, Soden B, Frush KS, Lowry C. Improved pediatric multidetector body CT using a size-based color-coded format. AJR Am J Roentgenol 2002;178(3):721–726.

19. Singh S, Kalra MK, Moore MA, et al. Dose reduction and compliance with pediatric CT protocols adapted to patient size, clinical indication, and number of prior studies. Radiology 2009;252(1):200–208.